Available online at www.sciencedirect.com

SCIENCE DIRECT®

Developmental Biology 271 (2004) 98–108

DEVELOPMENTAL BIOLOGY

www.elsevier.com/locate/ydbio

Real-time analysis of ureteric bud branching morphogenesis in vitro ☆

Tomoko Watanabe and Frank Costantini *

Department of Genetics and Development, Columbia University, New York, NY 10032, USA

Received for publication 19 February 2004, revised 30 March 2004, accepted 30 March 2004

Available online 6 May 2004

Abstract

While it is clear that the normal branching morphogenesis of the ureteric bud (UB) is critical for development of the metanephric kidney, the specific patterns of branching and growth have heretofore only been inferred from static images. Here, we present a systematic time-lapse analysis of UB branching morphogenesis during the early development of the mouse kidney in organ culture. Metanephric primordia from Hoxb7/GFP transgenic embryos were cultured for 3–4 days, and GFP images of the UB taken every 30 min were assembled into movies. Analysis of these movies (available as supplementary materials) revealed that the UB is a highly plastic structure, which can branch in a variety of complex patterns, including terminal bifid, terminal trifid, and lateral branching. To examine kinetic parameters of branching and elongation, skeletal representations of the UB were used to measure the number of segments and branch points and the length of each segment as a function of time and of branch generation. These measurements provide a baseline for future studies on mutant kidneys with defects in renal development. To illustrate how these quantitative methods can be applied to the analysis of abnormal kidney development, we examined the effects of the MEK1 inhibitor PD98059 on renal organ cultures and confirmed a previous report that the drug has a specific inhibitory effect on UB branching as opposed to elongation.

Keywords: Kidney development; Ureteric bud; Branching morphogenesis; Organ culture; Metanephric kidney; Green fluorescent protein; Erk MAP kinase

Introduction

The branching morphogenesis of an epithelial tube is a fundamental process that occurs during the development of parenchymal organs (Davies, 2002; Gilbert, 1997; Hu and Rosenblum, 2003). During organogenesis of the vertebrate metanephric kidney, the epithelial ureteric bud (UB) undergoes branching morphogenesis, under the control of factors produced by the surrounding metanephric mesenchyme and stromal cells, to give rise to the urinary collecting system (collecting ducts, calyces, pelvis, and ureter). The ureteric bud first arises as an outgrowth from the posterior end of the Wolffian duct, which grows into the adjacent mesenchyme where it begins to branch repeatedly while it continues to elongate. The correct pattern and extent of branching morphogenesis by the ureteric bud is critical for normal kidney development. Mutations that impair this process, either directly or indirectly, can result in renal agenesis or severe structural renal malformations that impact greatly on the regulatory functions of the kidney (Al-Awqati and Goldberg, 1998; Pohl et al., 2002).

Over the past decade, there have been significant advances in our understanding of the genetic control of kidney development, largely through studies using knockout and transgenic mice (Carroll and McMahon, 2003; Pohl et al., 2000; Vainio and Lin, 2002). To fully interpret the rapidly growing pool of genetic data, there is an increasing need for a more thorough and detailed description of the normal morphological events that occur during kidney development. Most of our ideas about the process of renal branching morphogenesis have been inferred from analysis of kidneys that were dissected and examined at a fixed stage of development, either at different gestational ages in vivo (e.g., Oliver, 1968) or after different times of organ culture in vitro (e.g., Cullen-McEwen et al., 2002; Lin et al., 2001, 2003). The branched structure of the ureteric "tree" has been visualized by a variety of methods, including histo-

☆ Supplementary data associated with this article can be found, in the online version, at doi:10.1016/j.ydbio.2004.03.025.

* Corresponding author. Department of Genetics and Development, Hammer Health Sciences Center, College of Physicians and Surgeons, Columbia University, Rm. 1602, 701 West 168th Street, New York, NY 10032. Fax: +1-212-923-2090.

E-mail address: fdc3@columbia.edu (F. Costantini).

0012-1606/$ - see front matter © 2004 Elsevier Inc. All rights reserved.
doi:10.1016/j.ydbio.2004.03.025

logical sectioning, confocal microscopy of whole kidneys stained with markers specific to the ureteric bud epithelium (which is most useful at early stages when the kidney is relatively small and transparent), or microdissection of the collecting ducts (particularly at later stages of organogenesis). While these methods can provide an accurate picture of the state of branching at any given time, they cannot unambiguously describe the sequence of morphogenetic events that gave rise to a particular structure. For example, the occurrence of two major modes of branching, terminal branching of the ampulla and lateral branching from within a preexisting trunk segment, cannot be distinguished retrospectively because the same branched structure could be formed by a variety of branching and elongation patterns (Fig. 1).

To define the sequence and kinetics of morphogenetic events, it is necessary to perform prospective time-lapse imaging as the organ develops. For the early stages of kidney development, time-lapse studies are feasible because metanephric kidney rudiments can be isolated and cultured in vitro (Grobstein, 1953; Saxen, 1987). The ability to visualize clearly the ureteric bud branches in a living kidney is a more recent advance, made possible by the development of a strain of transgenic mice that expresses the green fluorescent protein (GFP) in the ureteric bud (Srinivas et al., 1999). We have previously reported that in Hoxb7/GFP transgenic embryos, the GFP protein is expressed strongly throughout the Wolffian duct, the UB, and their derivatives and can easily be detected in living or fixed tissue. We described preliminary time-lapse studies that documented the occurrence of lateral as well as terminal branch formation in the developing kidney (Srinivas et al., 1999). In this study, we present a systematic time-lapse analysis of UB branching morphogenesis during the early development (first 70 h) of the mouse kidney in organ culture. This analysis reveals a variety of branching modalities that occur in normal cultured kidneys and defines a set of kinetic parameters that can form a baseline for future studies with various types of mutant kidneys. In addition, to illustrate how these methods can be applied to the analysis of abnormal kidney development, we have confirmed and quantified the effects of an inhibitor of the ras/MAP kinase-signaling cascade on UB branching (Fisher et al., 2001).

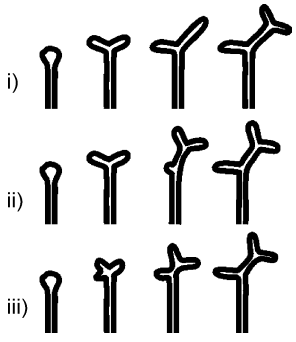

Fig. 1. Ambiguous origin of branched structures. Schematic diagrams of three possible sequences of branching and growth events, each of which can cause the same branched structure: (i) terminal bifid branching followed by unequal growth of the two daughter segments and bifid branching of only one daughter segment; (ii) terminal bifid branching followed by lateral branching within the trunk; (iii) terminal trifid branching, followed remodeling of the ampulla to yield two distinct branch points (“unequal trifid branching,” see text and Figs. 2 and 3).

Materials and methods

Organ culture of transgenic kidneys

These studies used the Hoxb7/EGFP transgenic line #33 that was previously described (Srinivas et al., 1999). Kidneys were dissected from E11.5 embryos in CO_2-independent medium (Invitrogen) and cultured on Transwell Clear filter units (Costar). The kidneys were then cultured in DMEM (Invitrogen) containing 10% fetal bovine serum and 50 μg/ml penicillin–streptomycin at 37°C in the presence of humidified 5% CO_2. In some cultures, the MEK1 inhibitor PD98059 (NEB, 9900S) was added to the same medium at a concentration of 50 μM (Fisher et al., 2001; Kashimata et al., 2000). The medium was changed every 1–2 days.

In one experiment, four kidneys were analyzed during simultaneous culture in normal medium (kidneys F, G, H, and I). In a separate experiment, five kidneys (kidneys A, B, C, D, and E) were analyzed during culture in normal medium and four (J, K, L, and M) during simultaneous culture in the presence of PD98059. For analysis of normal parameters of growth and branching, we combined the data from the two sets of kidneys grown in normal medium (kidneys A–E and F–I). To examine the effects of the MEK1 inhibitor, we compared kidneys J–M with kidneys A–E, all of which were cultured simultaneously. We excluded kidneys F–I from this comparison because they grew slightly more rapidly than kidneys A–E (data not shown).

Fluorescence microscopy and time-lapse imaging

Transwell filter units were placed inside a closed culture chamber that was attached to a prior automated X–Y–Z stage on a Nikon TE300 inverted microscope equipped for epifluorescence. The culture chamber had a clear top and bottom to allow imaging, six wells to hold the Transwell filter units, temperature control, and ports for the introduction and exhaust of humidified 5% CO_2. Movement of the automated stage to photograph each kidney culture in sequence, shutters to control the illumination of the specimens, and image acquisition were controlled by a computer running Windows NT and SimplePCI software (Compix, Inc.). Digital photographs (150 dpi, 1280 × 1024 pixel grayscale TIF files) of each kidney were taken at 30 min intervals, using an EGFP filter set (HYQ-GFP, Ex560/4,

Chroma-41001) and a Hamamatsu Orca digital CCD camera. To generate time-lapse movies, the resolution of each image was reduced to 75 dpi, cropped to center the growing kidneys using Adobe Photoshop, and the still images were converted to QuickTime format using GraphicConverter software or QuickTime Pro.

Image analysis

Each TIF image chosen for analysis (e.g., Fig. 2A) was inverted to a negative image using Adobe Photoshop; converted from grayscale to binary (Fig. 2B) using NIH Image (http://rsb.info.nih.gov/nih-image/index.html); and then converted to a skeleton (Fig. 2C) using NIH Image. The skeletons were color coded (Fig. 2D) to indicate branch generations. The number of segments (for each branch generation), length of each segment, number of tips, and number of branch points were measured for each selected image. To classify branching events as bifid vs. trifid vs. lateral, information from the skeletonized images was reconfirmed by examining additional time points in the movies.

Results

Normal kidney culture and analysis

To define the normal parameters of ureteric bud branching morphogenesis during kidney development in organ culture, we analyzed the growth of nine transgenic Hoxb7/GFP kidneys dissected from E11.5 embryos (designated "A" through "I"). The kidneys were cultured for 80–100 h and photographed for GFP fluorescence every 30 min. The images were assembled into QuickTime movies (QuickTime player is available for download at http://www.apple.com/quicktime/). Copies of movies are available online Supplementary Material.

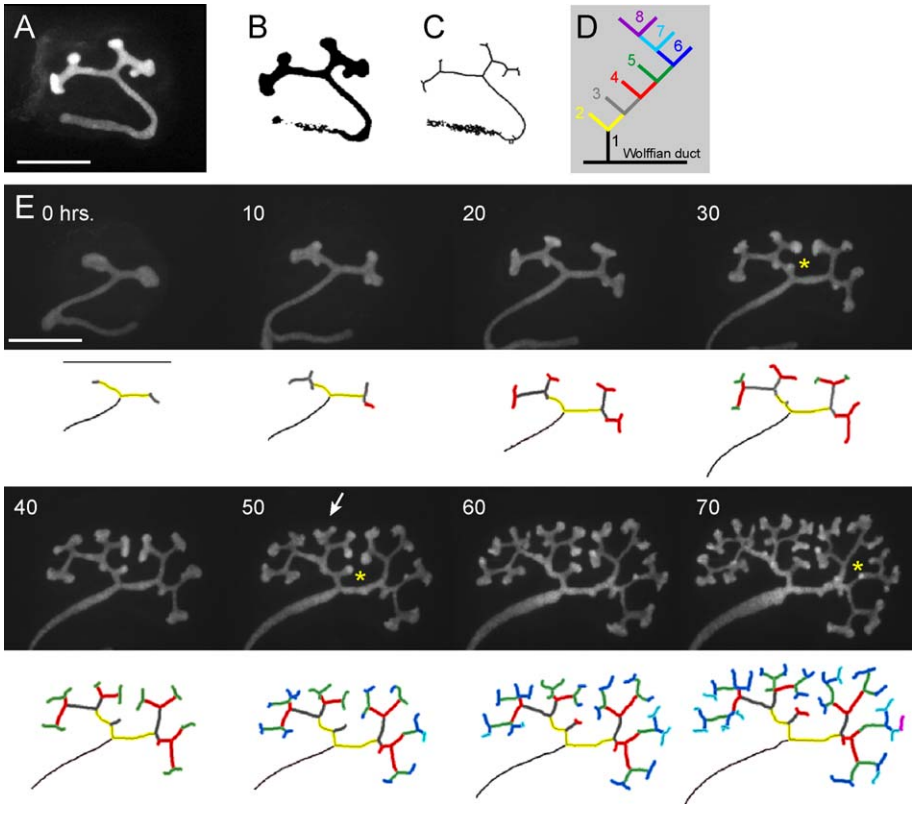

Fig. 2. Analysis of normal parameters of branching morphogenesis. (A–C) Image processing. Each grayscale image of GFP fluorescence (A) was converted to a negative binary image (B) and then to a skeletal representation (C). (D) Color code used to indicate the generation of branches according to the following conventions: the primary bud from the Wolffian duct is considered the "first generation" (black); the first two branches that form from the primary bud are the second generation (yellow); the third generation is dark gray; fourth generation, red; fifth generation, green; sixth generation, dark blue; seventh generation, light blue; and eighth generation, purple. (E) Example of a Hoxb7/GFP kidney (kidney "F") harvested at E11.5 and cultured in normal medium. GFP fluorescence images are shown at 10-h intervals. Below the GFP images are skeletonized, color-coded images of the ureteric bud, which were used for measurements of growth and branching. The white arrow at 50 h indicates an example of an unequal trifurcation, which gives rise to two distinct branch points by 70 h (shown at higher magnification in Fig. 3D). The yellow asterisks in E at 30 and 50 h indicate a lateral branch that subsequently bifurcates. The yellow asterisk in E at 70 h indicates a branch that is forming above or below the parental branch and is visible as a spot of increased GFP fluorescence. Scale bars = 500 μm.

To measure kinetic parameters of branching morphogenesis, eight images of each culture, at 10 h intervals (from 0 to 70 h), were analyzed in detail. Each image of the UB was converted to a stick figure or "skeleton" (see Materials and methods), and the branches were color coded to indicate their generation (Fig. 2). The initial bud that evaginated from the Wolffian duct (i.e., the presumptive ureter) was considered the "first generation" of branching, the next two branches forming the characteristic T-shaped structure were considered the "second generation," and so on. Since the second generation branches had already formed by the time the kidneys were dissected at E11.5 and the time of emergence of the third generation varied somewhat from kidney to kidney, the latter time was defined as "time 0" to synchronize the measurements between different kidneys. The analysis was terminated at 70 h because there was very little UB growth after this time, presumably due to limitations of the culture conditions.

The following terms will be used in our analysis of ureteric bud branching:

Segment. A length of UB bounded either by two branch points (trunk segment) or by one branch point and one tip (terminal segment).
Branch. A segment and any of the more distal segments that are connected to it.
Branch point. The point at which three or more segments connect.
Tip. The distal end of a terminal segment.
Ampulla. The swelling at the tip of a terminal segment.
Distal. Towards the tips, away from the Wolffian duct.
Proximal. Away from the tips, towards the Wolffian duct.

Diversity of branching events observed

The characteristic pattern of branching of the ureteric bud is usually described as a terminal bifurcation (Lin et al., 2003; Oliver, 1968; Saxen, 1987), and this was the most common type of branching event observed in our studies (Table 1). Most bifurcations were symmetrical: an ampulla first formed by the expansion of the UB tip and then extended in two directions at a similar rate (e.g., Figs. 2E and 3A). However, some terminal bifurcations were asymmetrical; in these cases, the ampulla first started to bulge in one lateral direction, typically at about 90° from the parental segment and only later began to produce a second bulge in the opposite direction (Fig. 3B). Regardless of the degree of symmetry, each bifurcation (by definition) ultimately resulted in two new terminal segments joined to the parental segment at a single branch point.

Table 1
Average occurrence of different types of branching events in each of the nine normal kidney cultures

Parental segment generation[a]	1st	2nd	3rd	4th	5th	6th	7th	Total
Generation formed by event	2nd	3rd	4th	5th	6th	7th	8th	
Type of branching event								
Terminal bifid	1.0	1.0	4.4	7.7	10.3	3.2	0.3	28.0 (75%)
Terminal trifid	0.0	1.0	1.0	2.6	1.9	0.1	0.1	6.7 (18%)
Lateral	0.0	1.6	0.7	0.2	0.0	0.0	0.0	2.4 (6%)
Total	1.0	3.6	6.1	10.3	12.1	3.3	0.7	37.1

[a] That is, the generation of the segment that causes the indicated type of branching event.

In addition to terminal bifurcation, other modes of branching were observed at significant frequencies. In approximately 18% of branching events, a single ampulla gave rise to three new terminal segments joined to the parental segment. These "trifid" branching events occurred most frequently during the third generation of branching (i.e., they formed from ampullae at the tips of second generation branches), where they accounted for half of the terminal branching events (Table 1). They were also frequently observed during the fourth, fifth, and sixth branch generations. While they appeared to be less common in later generations, this may be because the seventh and eighth generations did not develop fully by the end of the culture period, and the trifid branching properties of some ampullae may not yet have become apparent.

Some trifid branch points retained their trifid character over time, so that the three new terminal segments remained joined to the parental trunk segment at a common branch point (e.g., Fig. 3C). However, many of the trifid branch points were subsequently "remodeled" to give rise to two distinct bifid branch points (e.g., Figs. 3D and E). In these cases, one of the three new terminal segments arising from the ampulla grew out more slowly than the other two and its branch point shifted to a more proximal position on the parental trunk; meanwhile, the other two terminal segments grew faster and the branch point between them shifted to a more distal position. These were termed "unequal trifid" branching events. The distinctions between these various categories of terminal branching events (unequal vs. equal trifid, symmetrical vs. asymmetrical bifid, or unequal trifid vs. two successive bifids) were not always clear cut and they fell more into a continuum than into discrete classes. The diversity of branching patterns is most easily appreciated by viewing the time-lapse movies.

Another, more distinct category of branching events was lateral branching, defined as the outgrowth of a new terminal segment from the side of an existing segment rather than from the terminal ampulla (Figs. 2E and 3F) (Srinivas et al., 1999). These accounted for 6% of all branching events and almost always arose from the second or third generation segments (Table 1).

The daughter segments derived by terminal bifurcation, terminal trifurcation, or lateral branching displayed about the same relative frequency of bifurcation (approximately 80%) vs. trifurcation (approximately 20%) at their tips. Fig. 2E includes an example of a lateral branch that went on to

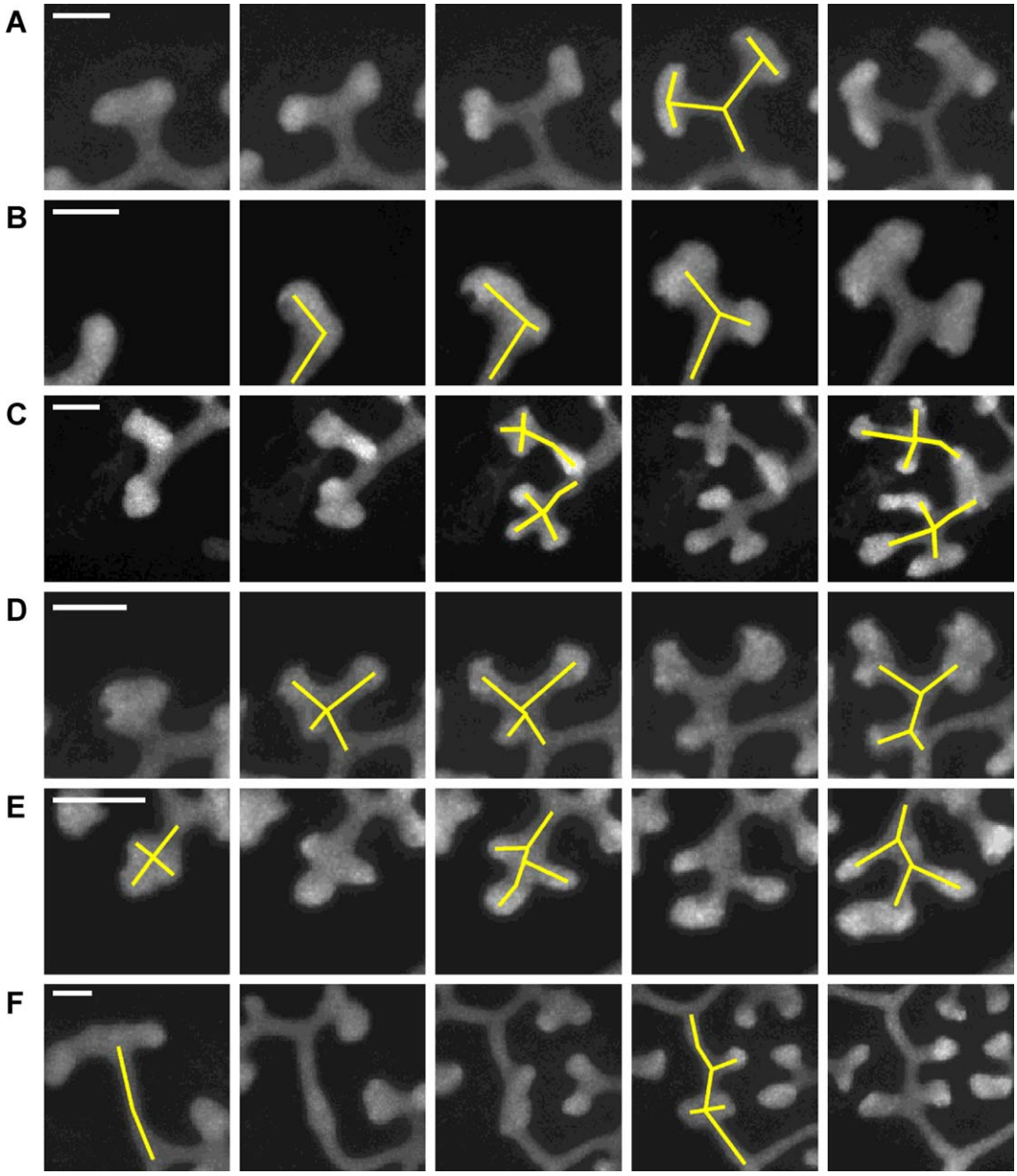

Fig. 3. Different modes of branching observed in time-lapse studies. The yellow stick drawings show an interpretation of the branching patterns. (A) Symmetrical terminal bifurcation. This example shows two tips, the products of a previous terminal bifurcation, each of which undergoes a subsequent symmetrical bifurcation. (B) Nonsymmetrical terminal bifurcation. The left branch appears first and grows more rapidly than the right branch. (C) Two examples of trifid branching, in which a single ampulla gives rise to three new branches. In each of these cases, the three daughter segments remain connected to the parental segment at a common branch point. (D and E) Two examples of unequal trifid branching. As in C, a single ampulla gives rise to three daughter segments, but what initially appears as a single branch point is gradually remodeled to produce two distinct branch points. (F) Lateral branching. This example shows the de novo formation of three lateral branches from the side of a trunk segment rather than from a terminal ampulla. Scale bars = 100 μm. Time spans shown: A, kidney C 34–70 h; B, kidney G 21–50 h; C, kidney E 39–75 h; D, kidney F 41–76 h; E, kidney G 74–106 h; and F, kidney A 20–95 h.

branch in a bifid manner at its tip. Thus, the propensity of a segment to branch in a certain pattern is not apparently influenced by the mode of branching by which it arose.

Kinetic parameters of growth and branching

For each of the 72 skeletons (nine kidneys, eight time points each), we counted the number of branch points and segments and measured the length of each segment. These data were analyzed first for the entire kidney (Fig. 4) and then separately for each branch generation (Fig. 5). The aggregate length of the UB tree (i.e., the sum of the lengths of all the segments) increased by approximately 13-fold over the 70-h period of analysis (Fig. 4A). The rate at which the aggregate length increased (i.e., the total elongation rate) started at 40 μm/h, increased steadily to 120

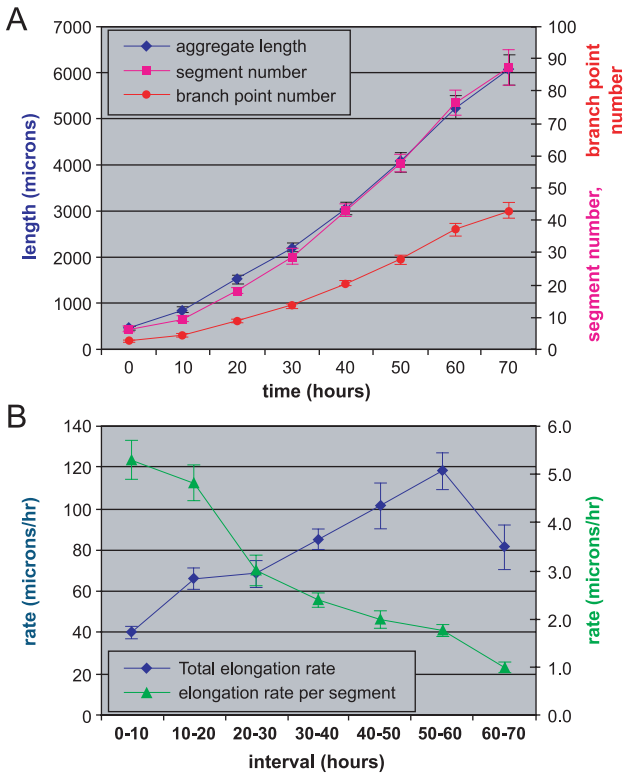

Fig. 4. Kinetics of ureteric bud elongation and branching. (A) Aggregate length of the entire ureteric bud tree and total number of branch point and segments during 70 h of culture. (B) Elongation rate of the entire ureteric bud tree ("total elongation rate") and elongation rate of the average UB segment. The data in A and B are the sum of the second through eighth branch generations—the first generation (the presumptive ureter) was not included. Data shown are the mean ± SE for nine E11.5 kidneys cultured in normal medium.

μm/h by 50–60 h, and then decreased somewhat (Fig. 4B). The average number of branch points increased from about 3 to 43 (Fig. 4A) and the average number of segments from 6 to 87 (Fig. 4A). By dividing the rate of total elongation in each 10-h interval by the average number of segments present during that interval, we could estimate the average rate of elongation per segment (Fig. 4B). This rate started at 5.3 μm per h and decreased continuously to 1.0 μm/h by 60–70 h of culture. The decrease is due largely to a slowing of growth of the earlier branch generations (see below).

An examination of growth parameters for each individual branch generation provided a more detailed view of the kinetics of branching morphogenesis. Fig. 5A shows the aggregate length of each branch generation, Fig. 5B the number of segments, and Fig. 5C the average segment length for each generation. At time 0 (by definition), the second generation segments had all formed and they had just begun to branch at their tips. They continued to elongate, increasing about twofold in length during the next 70 h (average growth rate 2.2 μm/h). The third generation segments had mostly appeared at time 0, but their number increased somewhat during the next 70 h (Fig. 5B); part of this increase was due to the emergence of third generation lateral branches from within the second generation branches (Table 1 and Fig. 2E; 30 h). The fourth generation segments elongated rapidly for the first 20 h (at approximately 5 μm/h), but their average length reached a plateau by about 30 h (Fig. 5C). The later generations of segments also showed a relatively high initial growth rate, followed by a period of

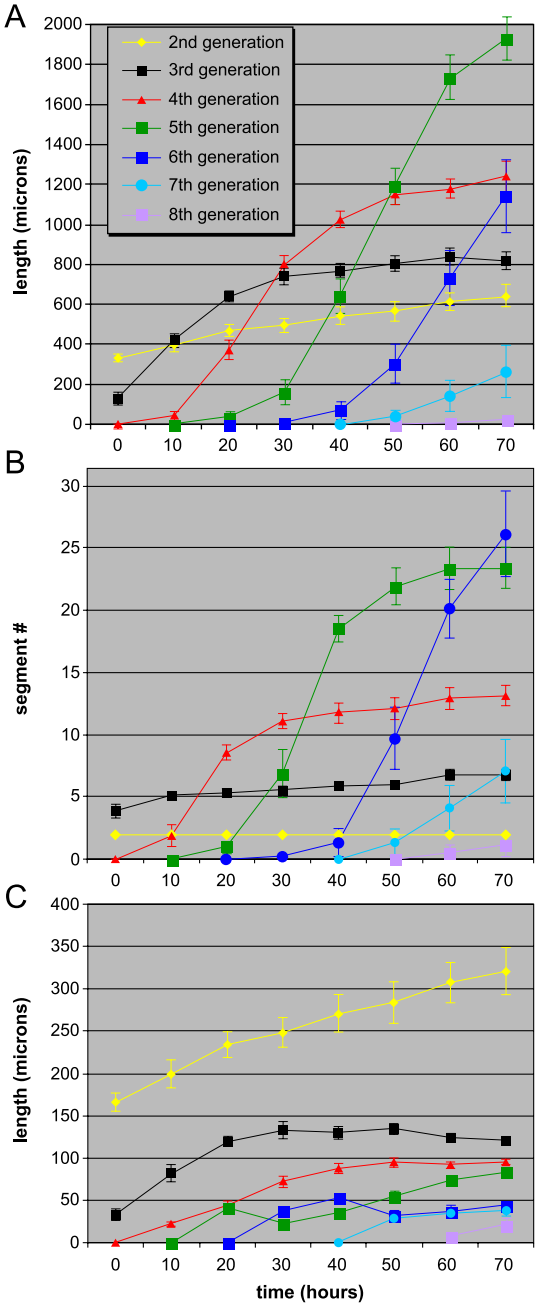

Fig. 5. Kinetics of elongation of the ureteric bud as a function of branch generation. (A) Aggregate length of all the segments of the second through eighth generations (color code as described in Fig. 2). (B) Number of segments of each generation. (C) Average length of the segments of each generation. Data shown are the mean ± SE for nine E11.5 kidneys cultured in normal medium.

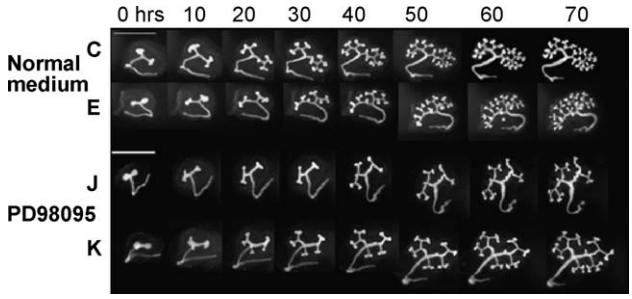

Fig. 6. Time-lapse GFP images of E11.5 kidneys cultured with or without the MEK1 inhibitor PD98059. Top, images of kidneys C and E cultured in normal medium for the indicated number of h. Bottom, kidneys J and K cultured in the presence of 50 μM PD98059. Scale bars = 1 mm. The asterisk in kidney E at 60 h indicates a new branch forming above or below the parental branch, which is visible as a spot of increased GFP fluorescence.

slower growth (Fig. 5C). This was consistent with our subjective impression (from examination of the time-lapse movies) that new terminal segments elongated at a higher rate until they branched at their tips, after which they grew more slowly.

The successive generations of branches appeared in a regular and sequential (although not strictly synchronous) fashion (Fig. 5B): most fourth generation segments appeared between 10 and 30 h, the fifth generation between 20 and 40 h, and the sixth generation after 40 h, seventh generation after 50 h, and the eighth generation after 60 h. There was also a regular hierarchy in the final length achieved by each generation of segments (Fig. 5C): sixth generation segments remained shorter than fifth generation segments, which remained shorter than fourth generation, and so on.

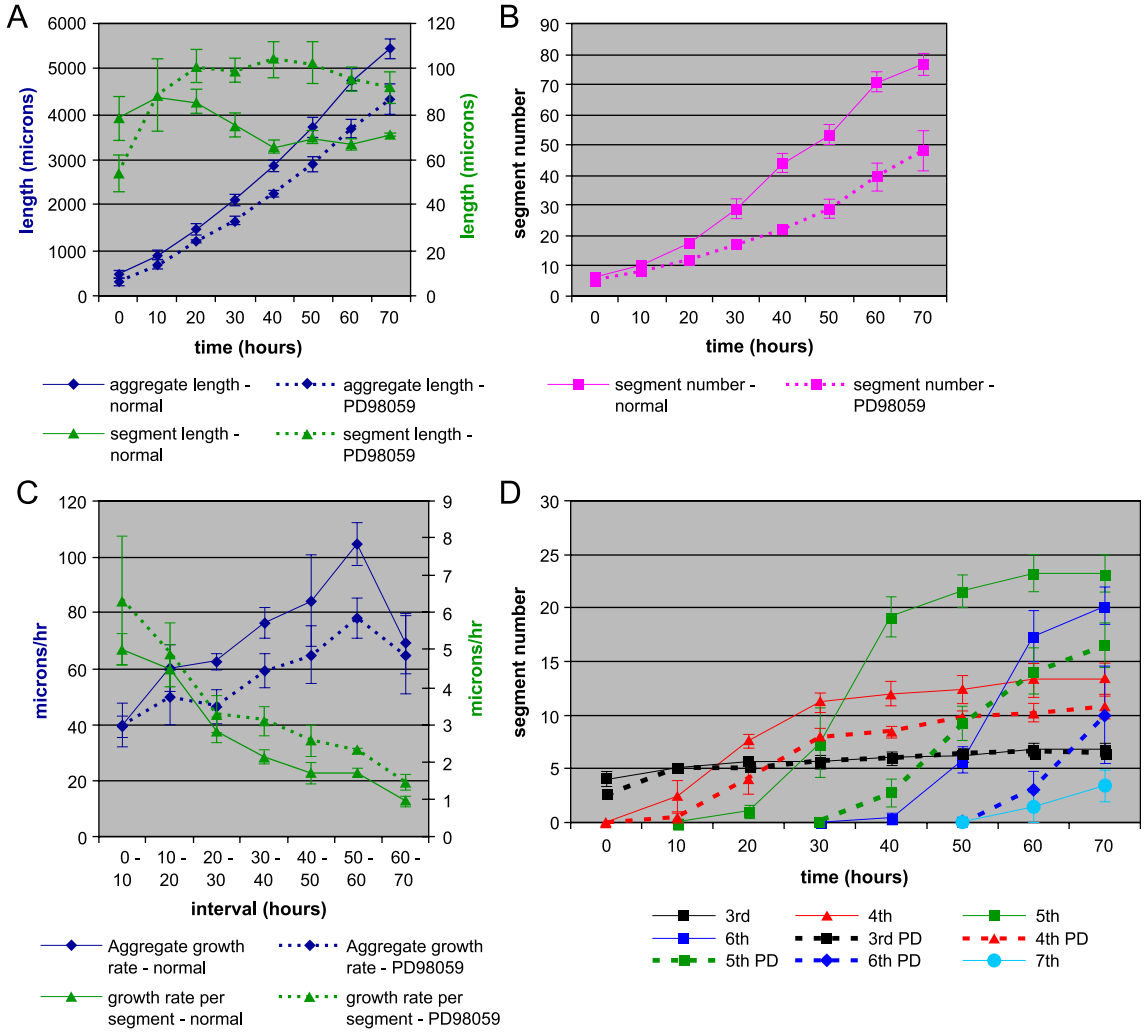

Fig. 7. Effect of the MEK1 inhibitor PD98059 on the kinetics of ureteric bud elongation and branching. (A) Aggregate length of the ureteric bud and average length per segment between 0 and 70 h of culture. (B) Total number of segments. (C) Elongation rate of the entire ureteric bud and elongation rate of the average segment. (D) Number of segments of the third through seventh generations. Data shown are average ± SE for five normal kidneys, solid lines (A–E) and four PD98059-treated kidneys, dashed lines (J–M). Kidneys A–E and J–M were cultured simultaneously.

Analysis of the effects of a MEK1 inhibitor on the rate of ureteric bud branching and elongation

To illustrate the utility of these methods for quantitating the effects of drugs or mutations that alter the kinetics of branching morphogenesis, we conducted the same measurements on four E11.5 kidneys that were cultured in the presence of the drug PD08059. PD98059 specifically blocks the phosphorylation of Erk 1/2 by the MEK1 MAP kinase kinase and thus blocks this MAP kinase-signaling cascade (Alessi et al., 1995; Kashimata et al., 2000). We confirmed the efficacy of the drug in our experiments by examining the phosphorylation of Erk 1/2 in kidneys cultured for 3 days ± PD98059 by Western blotting using anti-phospho-ERK1/2 antibodies (data not shown). Fisher et al. (2001) have reported that the Erk 1/2 MAP kinase is normally active in the ureteric bud and that inhibiting its activation with PD98059 reduces ureteric bud branching while allowing elongation to continue. As illustrated in Fig. 6, we also observed a reduction in branching of the UB, at a qualitative level, in the PD98059-treated cultures. This was further substantiated by quantitative measurements (Fig. 7).

The aggregate elongation rate for the entire ureteric bud tree was only slightly depressed in the kidneys cultured with PD98059, in comparison to the controls (Fig. 7A), and the final aggregate length at 70 h was 79% of the control value. However, the average number of segments at 70 h, one measure of the rate of branching, was only 62% of the control value (Fig. 7B). The reduced amount of branching in the presence of PD98059 was also apparent from two other parameters: the length of the average segment (Fig. 7A) and the elongation rate of the average segment (Fig. 7C). In the controls, the average segment length varied only slightly during the growth of the kidneys and stabilized at about 70 μm (Fig. 7A) (this reflects a balance between the elongation of existing segments and the birth of new, initially short segments). In contrast, the average segment length of the PD98059-treated kidneys reached a significantly higher value (90–100 μm) (Fig. 7A), and the growth rate of the average segment was also consistently elevated in the presence of the drug (Fig. 7C). Thus, the effect of the MEK1 inhibitor is apparently to favor elongation at the expense of branching.

The retardation in branching caused by PD98059 was also reflected in the timing with which each generation of segments appeared (Fig. 7D). The appearance of the fourth generation was delayed by about 5–10 h compared to controls, the fifth and sixth generations were delayed by 15–20 h, and the seventh generation had not appeared by the end of the experiment.

Despite the reduced rate of branching, there was no significant effect of the inhibitor on the types of branching events observed. Terminal trifurcation occurred at a frequency of 14% and lateral branching at a frequency of 8%. As in control kidneys, lateral branches grew most frequently from the second generation segments, while terminal trifurcations continued to occur over several generations of branching (data not shown).

Discussion

Morphogenesis is a four-dimensional process: three dimensions in space and one in time. Yet, for mammalian development, which normally occurs in utero, much of our knowledge of morphogenetic processes relies on observations at a single point in time, from which we can only try to infer the preceding developmental events. In the case of the kidney, the ability of the organ primordium to develop in culture for several days permits the continuous, real-time observation of the same specimen throughout its development, at least for the early stages of organogenesis. However, in a growing kidney in organ culture, the thickness of the tissue and the diversity of cell types make it difficult to visualize many aspects of morphogenesis, including the branching of the ureteric bud epithelium, which is normally obscured by the overlying mesenchyme and its epithelial derivatives. Here we have made use of a transgenic mouse line that expresses GFP in the ureteric bud (Srinivas et al., 1999), in combination with organ culture and time-lapse imaging techniques, to provide the first real-time kinetic analysis of ureteric bud branching morphogenesis.

In addition to permitting direct measurements of the rates of tubule elongation and branching, these studies have provided new insight into the diversity of ureteric bud branching patterns. We observed two general types of branching: lateral and terminal. Lateral branching accounted for 6% of all branching events and occurred almost exclusively from the early (second and third) generations of branch segments. While lateral branching of the ureteric bud has been previously inferred from static observations (Lin et al., 2001, 2003; Oliver, 1968), lateral branches cannot be definitively identified after they have occurred because the same structure generated by a lateral branch can also result from a terminal branching event followed by unequal growth of the daughter segments (Fig. 1).

It is not clear why lateral branches occurred only from the earlier generations of segments. One possibility is that only longer segments can form lateral branches: the shortest segment to form a lateral branch was over 100 μm in length (data not shown) and most segments of the later generations never reached this length (Fig. 5C). Alternatively, the ability of early generation segments to form lateral branches could be due to their age, their state of differentiation, or their more central location within the developing kidney, in contrast to later generation segments, which are generally closer to the periphery. The ability to clearly distinguish lateral branches should make it easier to study the factors that control their formation and to

determine if different mechanisms control lateral vs. terminal branching of the UB.

The more common terminal mode of branching showed a considerable degree of complexity. All terminal branching begins with the formation of a swollen ampulla at the tip. The ampulla typically expands to two or three times the diameter of the parental trunk before it is clear how many daughter segments it will produce. In the case of a symmetrical bifid branching event, the ampulla flattens and extends in two opposite directions to form the characteristic "T" structure. In other cases (asymmetrical bifid branching), the ampulla first grows in one direction, forming an L rather than a T, and only later does the opposite new segment emerge. In the case of trifurcation, the ampulla gives rise to three distinct bumps, each of which forms a new terminal segment. These sometimes grow out at the same rate, but more commonly two grow faster and the third more slowly. Most of the resulting trifid branch points are transient structures: as the three new branches grow out, the point of attachment of the slower growing branch separates from the original branch point so that the resulting structure resembles the product of two successive bifid branching events, or a bifid plus a lateral branch (Fig. 1). Overall, our time-lapse analysis revealed that the ampulla is a highly plastic structure that can be extensively remodeled to cause a variety of branched structures.

Trifid branching has been noted in some previous studies of UB branching, but not in others. Lin et al. (2001, 2003), who examined the UB of E11.5 kidneys cultured for various time periods and stained with an epithelial marker, reported an 88% frequency of terminal bifid branching and 12% frequency of lateral branching. Given our results, it is likely that some of the apparently lateral branches in this study had actually been produced by an unequal terminal trifurcation. On the other hand, Oliver (1968), who performed extensive microdissection of human kidneys at different stages of gestation, noted the presence, early on, of some irregularly shaped ampullae suggesting an incipient trifid division. Furthermore, Oliver (1968) deduced that these structures were later remodeled because only bifid branch points were observed in the collecting ducts at later stages of gestation. Majumdar et al. (2003) have also noted the high frequency of trifurcations during the formation of the third branch generation in mouse kidneys.

In general, the occurrence of different types of terminal branching events could not be predicted from the developmental history of a particular segment. Lateral branching did not alternate in a regular manner with terminal bifid branching, as in one suggested model for UB branching (Al-Awqati and Goldberg, 1998). However, the observed patterns of UB branching had several regular features. The first branching event (formation of second generation branches) was always bifid and the next generation was very often trifid (Table 1). As noted above, lateral branching almost always occurred from second or third generation branches, although the specific locations of the lateral branches and times at which they emerged were variable. There was a degree of regularity in the appearance of successive branch generations (Fig. 5B) and a clear hierarchy in the final length achieved by each generation of segments (Fig. 5C). Therefore, while the specific branching pattern of each kidney was unique and not entirely predictable, neither was entirely random.

These time-lapse studies allowed us to calculate accurately the rates of ureteric bud elongation and branching. The total length of the ureteric bud increased by more than 13-fold during over 70 h, and the number of branch points and segments also increased by a similar amount (Fig. 4A). In a recent study, Cullen-McEwen et al. (2002) studied the growth of the UB by culturing E12 mouse kidneys for different periods of time ranging from 6 to 48 h, then fixing and staining the kidneys; they then used confocal microscopy to measure the lengths and branch point numbers of the ureteric buds. If we take into account the fact that the kidneys in our study were dissected 1 day earlier, both sets of values for the rate of increase in total length and branch point numbers are quite comparable. Both sets of data indicate that the length of the average ureteric bud segment remains fairly constant as the kidney grows over several days (Fig. 7A). However, this average does not reflect the growth of individual segments. A more detailed view of growth was obtained in the present study by analyzing independently each generation of branch segments (Fig. 5). This showed that each generation displays an early phase of rapid growth, followed by a longer phase of slower growth.

We were able to confirm, in a quantitative manner, the conclusions of an earlier study (Fisher et al., 2001) showing that the MEK1 inhibitor PD98059 specific inhibits ureteric bud branching and has less of an effect on overall growth. The rate of branching (as measured by the increase in number of segments; Fig. 7B) was reduced in the presence of the drug, while the elongation rate of the average segment was increased (Fig. 7C). As a consequence, the time interval between the appearance of each successive branch generation was considerably lengthened (Fig. 7D), as was the resulting average segment length (Fig. 7A). This drug blocks the activation of the MAP kinase kinase MEK1 (Alessi et al., 1995), which functions in a signal transduction pathway downstream of many growth factor receptors (Schlessinger, 2000). In the case of the kidney, several families of growth factors that are known to influence ureteric bud morphogenesis, including GDNF and FGFs, activate this pathway (Carroll and McMahon, 2003; Pohl et al., 2000; Szebenyi and Fallon, 1999; Takahashi, 2001; Vainio and Lin, 2002). It is not possible in such an experiment to determine which of these signaling pathways was responsible for the observed effects of the inhibitor. Nevertheless, this experiment illustrates the utility of the Hoxb7/GFP transgenic line, and the methods of time-lapse analysis we have employed here, to investigate the specific effects of different agents or mutations

that alter the process of ureteric bud branching morphogenesis.

It is important to point out some of the limitations of the current study and areas in which the technology could be improved. First, the standard kidney organ culture system results in the growth of the kidney in a relatively flattened form on a filter. This is beneficial in one respect because it allows the entire UB to be visualized in a single image obtained with a standard epifluorescence microscope. To better define the normal patterns of morphogenesis, it will be necessary to employ improved culture systems in which the three-dimensional structure of the kidney is maintained. In our image analysis, we treated the UB as a two-dimensional structure, which is a simplification. While most growth occurred in the X–Y plane, due to the flattened growth of the kidney on the filter, occasionally a new tip grew mainly in the Z-axis of the culture (i.e., straight up or down). These tips were clearly visible as spots of increased GFP fluorescence on the parental ampulla or trunk (see examples in Figs. 2 and 6), although their length and growth rate could not be determined. Methods are being developed for acquisition and analysis of three-dimensional images of the ureteric bud (Cullen-McEwen et al., 2002), which if combined with improved organ culture methods that retain three dimensionality will ultimately result in a more authentic picture of kidney growth. We also reduced our images of the ureteric bud to a skeletal form, treating the branches as linear structures. More refined methods of image analysis should ultimately provide a more detailed and accurate view of processes that cannot be reduced to skeletal form, such as the complex changes in the shape of the ampulla that cause new branches. The available in vitro culture systems are likely to underestimate the rates of growth that occurs in vivo; in particular, the reduction in growth rates that we observed towards the end of the 70-h period of analysis are likely to be an artifact of the culture system. However, it is likely that the specific features of ureteric bud branching we have described (e.g., the occurrence of lateral branching and the diversity of terminal branching patterns) reflect the in vivo situation. Finally, we have been limited to analyzing only the earliest stages of kidney development; a great many changes in the ureteric bud take place in vivo after the early stages that we have been able to analyze, giving rise to the complex form of the collecting system in the mature kidney. Improved methods of in vivo imaging will be necessary to accurately describe these processes.

Nevertheless, in vitro culture systems combined with the use of transgenic fluorescent protein markers offer a powerful approach for visualizing and understanding the early events in renal development. The development of different colors of fluorescent proteins, which can be visualized and distinguished in the same specimen (Hadjantonakis et al., 2003; van Roessel and Brand, 2002), and the generation of new transgenic mouse lines in which different cell types in the developing kidney are labeled should provide unprecedented insight into morphogenetic processes such as cell migration, mesenchymal to epithelial transitions, and cell differentiation.

Acknowledgments

We thank Hiroko Watanabe-Meserve (New York University School of Medicine) for assistance with statistical analysis, Gary Johnson (Center for Radiological Research) for construction of the culture chamber, and Doris Herzlinger and Cathy Mendelsohn for helpful comments on the manuscript. This work was supported by a grant from the NIDDK.

References

Al-Awqati, Q., Goldberg, M.R., 1998. Architectural patterns in branching morphogenesis in the kidney. Kidney Int., 54.

Alessi, D.R., Cuenda, A., Cohen, P., Dudley, D.T., Saltiel, A.R., 1995. PD 098059 is a specific inhibitor of the activation of mitogen-activated protein kinase kinase in vitro and in vivo. J. Biol. Chem. 270, 27489–27494.

Carroll, T.J., McMahon, A.P., 2003. Overview: the molecular basis of kidney development. In: Vize, P.D., Woolf, A.S., Bard, J.B.L. (Eds.), The Kidney. From Normal Development to Congenital Disease. Academic Press, Amsterdam, pp. 343–376.

Cullen-McEwen, L.A., Fricout, G., Harper, I.S., Jeulin, D., Bertram, J.F., 2002. Quantitation of 3D ureteric branching morphogenesis in cultured embryonic mouse kidney. Int. J. Dev. Biol. 46, 1049–1055.

Davies, J.A., 2002. Do different branching epithelia use a conserved developmental mechanism? BioEssays 24, 937–948.

Fisher, C.E., Michael, L., Barnett, M.W., Davies, J.A., 2001. Erk MAP kinase regulates branching morphogenesis in the developing mouse kidney. Development 128, 4329–4338.

Gilbert, S.F., 1997. Developmental Biology. Sinauer Associates Inc., Sunderland, MA.

Grobstein, C., 1953. Morphogenetic interaction between embryonic mouse tissues separated by a membrane filter. Nature 172, 869–871.

Hadjantonakis, A.K., Dickinson, M.E., Fraser, S.E., Papaioannou, V.E., 2003. Technicolour transgenics: imaging tools for functional genomics in the mouse. Nat. Rev. Genet. 4, 613–625.

Hu, M.C., Rosenblum, N.D., 2003. Genetic regulation of branching morphogenesis: lessons learned from loss-of-function phenotypes. Pediatr. Res. 54, 433–438.

Kashimata, M., Sayeed, S., Ka, A., Onetti-Muda, A., Sakagami, H., Faraggiana, T., Gresik, E.W., 2000. The ERK-1/2 signaling pathway is involved in the stimulation of branching morphogenesis of fetal mouse submandibular glands by EGF. Dev. Biol. 220, 183–196.

Lin, Y., Zhang, S., Rehn, M., Itaranta, P., Tuukkanen, J., Heljasvaara, R., Peltoketo, H., Pihlajaniemi, T., Vainio, S., 2001. Induced repatterning of type XVIII collagen expression in ureter bud from kidney to lung type: association with sonic hedgehog and ectopic surfactant protein C. Development 128, 1573–1585.

Lin, Y., Zhang, S., Tuukkanen, J., Peltoketo, H., Pihlajaniemi, T., Vainio, S., 2003. Patterning parameters associated with the branching of the ureteric bud regulated by epithelial-mesenchymal interactions. Int. J. Dev. Biol. 47, 3–13.

Majumdar, A., Vainio, S., Kispert, A., McMahon, J., McMahon, A.P., 2003. Wnt11 and Ret/Gdnf pathways cooperate in regulating ureteric branching during metanephric kidney development. Development 130, 3175–3185.

Oliver, J., 1968. Nephrons and Kidneys; A Quantitative Study of Developmental and Evolutionary Mammalian Renal Architectonics. Hoeber Medical Division Harper & Row, New York.

Pohl, M., Stuart, R.O., Sakurai, H., Nigam, S.K., 2000. Branching morphogenesis during kidney development. Annu. Rev. Physiol. 62, 595–620.

Pohl, M., Bhatnagar, V., Mendoza, S.A., Nigam, S.K., 2002. Toward an etiological classification of developmental disorders of the kidney and upper urinary tract. Kidney Int. 61, 10–19.

Saxen, L., 1987. Organogenesis of the Kidney. Cambridge Univ. Press, Cambridge.

Schlessinger, J., 2000. Cell signaling by receptor tyrosine kinases. Cell 103, 211–225.

Srinivas, S., Goldberg, M.R., Watanabe, T., D'Agati, V., al-Awqati, Q., Costantini, F., 1999. Expression of green fluorescent protein in the ureteric bud of transgenic mice: a new tool for the analysis of ureteric bud morphogenesis. Dev. Genet. 24, 241–251.

Szebenyi, G., Fallon, J.F., 1999. Fibroblast growth factors as multifunctional signaling factors. Int. Rev. Cytol. 185, 45–106.

Takahashi, M., 2001. The GDNF/RET signaling pathway and human diseases. Cytokine Growth Factor Rev. 12, 361–373.

Vainio, S., Lin, Y., 2002. Coordinating early kidney development: lessons from gene targeting. Nat. Rev. Genet. 3, 533–543.

van Roessel, P., Brand, A.H., 2002. Imaging into the future: visualizing gene expression and protein interactions with fluorescent proteins. Nat. Cell Biol. 4, E15–E20.